ISSN 1674-1056
http://cpb.iphy.ac.cn
http://iopscience.iop.org/cpb
中国物理 B
Chinese Physics
中国物理
Chinese Physics B

Designing solar-cell absorber materials through computational high-throughput screening

Xiaowei Jiang(江小蔚), Wan-Jian Yin(尹万健)
Citation: Chin. Phys. B . 2020, 29(2): 028803 . **doi:** 10.1088/1674-1056/ab6655
Journal homepage: http://cpb.iphy.ac.cn; http://iopscience.iop.org/cpb

What follows is a list of articles you may be interested in

The effect of Mn-doped ZnSe passivation layer on the performance of CdS/CdSe quantum dot-sensitized solar cells

Yun-Long Deng(邓云龙), Zhi-Yuan Xu(徐知源), Kai Cai(蔡凯), Fei Ma(马飞), Juan Hou(侯娟), Shang-Long Peng(彭尚龙)
Chin. Phys. B . 2019, 28(9): 098802 . **doi:** 10.1088/1674-1056/ab37f3

Exploring alkylthiol additives in PBDB-T:ITIC blended active layers for solar cell applications

Xiang Li(李想), Zhiqun He(何志群), Mengjie Sun(孙盟杰), Huimin Zhang(张慧敏), Zebang Guo(郭泽邦), Yajun Xu(许亚军), Han Li(李瀚), Chunjun Liang(梁春军), Xiping Jing(荆西平)
Chin. Phys. B . 2019, 28(8): 088802 . **doi:** 10.1088/1674-1056/28/8/088802

New design of ferroelectric solar cell combined with luminescent solar concentrator

Slimane Latreche, Mohamed Fathi, Abderrahmane Kadri
Chin. Phys. B . 2019, 28(8): 088801 . **doi:** 10.1088/1674-1056/28/8/088801

Effect of carrier mobility on performance of perovskite solar cells

Yi-Fan Gu(顾一帆), Hui-Jing Du(杜会静), Nan-Nan Li(李楠楠), Lei Yang(杨蕾), Chun-Yu Zhou(周春宇)
Chin. Phys. B . 2019, 28(4): 048802 . **doi:** 10.1088/1674-1056/28/4/048802

Self-assembled monolayer modified copper(I) iodide hole transport layer for efficient polymer solar cells

Yuancong Zhong(钟远聪), Qilun Zhang(张琪伦), You Wei(魏优), Qi Li(李琦), Yong Zhang(章勇)
Chin. Phys. B . 2018, 27(7): 078802 . **doi:** 10.1088/1674-1056/27/7/078802

TOPICAL REVIEW — High-throughput screening and design of optoelectronic materials

Designing solar-cell absorber materials through computational high-throughput screening*

Xiaowei Jiang(江小蔚)[1,2] and Wan-Jian Yin(尹万健)[1,2,3,†]

[1] College of Energy, Soochow Institute for Energy and Materials Innovations (SIEMIS), Soochow University, Suzhou 215006, China
[2] Key Laboratory of Advanced Carbon Materials and Wearable Energy Technologies of Jiangsu Province, Soochow University, Suzhou 215006, China
[3] Key Laboratory of Advanced Optical Manufacturing Technologies of Jiangsu Province & Key Laboratory of Modern Optical Technologies of Education Ministry of China, Soochow University, Suzhou 215006, China

(Received 19 November 2019; revised manuscript received 25 December 2019; accepted manuscript online 31 December 2019)

Although the efficiency of $CH_3NH_3PbI_3$ has been refreshed to 25.2%, stability and toxicity remain the main challenges for its applications. The search for novel solar-cell absorbers that are highly stable, non-toxic, inexpensive, and highly efficient is now a viable research focus. In this review, we summarize our recent research into the high-throughput screening and materials design of solar-cell absorbers, including single perovskites, double perovskites, and materials beyond perovskites. $BaZrS_3$ (single perovskite), Ba_2BiNbS_6 (double perovskite), $HgAl_2Se_4$ (spinel), and $IrSb_3$ (skutterudite) were discovered to be potential candidates in terms of their high stabilities, appropriate bandgaps, small carrier effective masses, and strong optical absorption.

Keywords: solar cell, high-throughput, materials design, first-principles calculations

PACS: 88.40.H–, 88.40.J–, 88.30.gg, 31.15.es **DOI:** 10.1088/1674-1056/ab6655

1. Introduction

Catalyzed by the energy crisis and environmental pollution from the consumption of fossil fuels, the quest for renewable and clean energy has driven the exploration and development of solar-cell materials.[1–5] As shown in Fig. 1, the first-generation solar cells were fabricated using silicon absorbers (1950s), while the second-generation solar cells were based on GaAs (1960s) and CdTe (1970s), while these cells exhibited good performance and extremely long-term stabilities,[6–8] their electronic properties were generally less tolerant to defects due to the covalent systems in which low defect concentrations usually significantly degraded the cell performance.[9,10] Therefore, high-quality crystals or post-treatment are required to passivate the dangling bonds.[11–14] Following the development of CdTe cells, a number of ionic compounds, such as $Cu_2(In, Ga)Se_4$ (1990s) and $Cu_2ZnSn(S, Se)_4$ (2000s), were discovered by chemically mutating cations. Due to their multinary nature, defect control is crucial to enhancing the efficiency, especially for $Cu_2ZnSn(S, Se)_4$.[15–23]

In the last decade, hybrid organic-inorganic perovskites, such as $CH_3NH_3PbI_3$ ($MAPbI_3$), have led to a new revolutionary class of solar-cell absorbers that produce inexpensive and highly efficient thin-film solar cells.[24–54] The certified photoconversion efficiencies (PCEs) of these materials are continually being refreshed at a high rate, from 3.8% in 2009[24] to 25.2% in 2019 (NREL Best Research-Cell Efficiency Chart, accessed November 2019). $MAPbI_3$ exhibits an appropriate direct bandgap, strong optical absorption, balanced electron and hole effective masses, long carrier lifetime and diffusion length, as well as shallow dominating defects.[8,35,41,42,55–59] These superior optical and electronic properties are mainly attributed to strong coupling between the lone-pair s orbital of Pb and the p orbital of I.[60,61] Despite these advantages, two major obstacles for the commercialization of $MAPbI_3$ exist: poor long-term stability and the toxicity of Pb,[43,62–64] which have propelled researchers to develop better materials with improved chemical stabilities and environmentally friendly compositions. One solution involves replacing the volatile organic MA molecule with elemental Cs.[65,66] Considering that the MA in $MAPbI_3$ does not obviously contribute to the overall electronic structure, the inorganic $CsPbI_3$ counterpart should exhibit similar material properties.[67–72] A $CsPbI_3$-based solar cell has been shown to deliver a PCE of 18.64%,[73] however it suffers from long-term phase instability as the Cs^+ is insufficiently large to sustain a stable perovskite structure, although recent work has shown that the $CsPbI_3$ perovskite phase can be stabilized by additional processes and passivation.[74–76]

*Project supported by the National Key Research and Development Program of China (Grant No. 2016YFB0700700), the National Natural Science Foundation of China (Grant Nos. 11674237, 11974257, and 51602211), the Priority Academic Program Development of Jiangsu Higher Education Institutions (PAPD), China, and the Suzhou Key Laboratory for Advanced Carbon Materials and Wearable Energy Technologies, China.

†Corresponding author. E-mail: wjyin@suda.edu.cn

© 2020 Chinese Physical Society and IOP Publishing Ltd

To tackle the Pb toxicity problem, the divalent Pb cation in $CsPbX_3$ has been mutated into monovalent B(I) and trivalent B(III) cations, which led to a class of halide double perovskite with the A_2B(I)B(III)X_6 formula.[77–82] While $Cs_2AgBiBr_6$ and $Cs_2AgBiCl_6$ were successfully synthesized in early 2016,[83–85] unfortunately $Cs_2AgBiBr_6$ has a bandgap ($\approx$ 1.9 eV)[83,86] that is slightly larger than the optimal bandgap range, it also exhibits indirect bandgaps owing to chemical mismatching of the Ag d and Bi s orbitals,[87] which results in a PCE much lower than that of $MAPbI_3$. So far, the highest reported PCE for $Cs_2AgBiBr_6$ is 2.5%.[88] Unfortunately, low-bandgap Cs_2AgBiI_6 is difficult to synthesize.[85] Cs_2AgInX_6 (X = Cl and Br), as other contenders, have been prepared and exhibit direct bandgaps, however, their optical bandgaps are too large owing to the parity-forbidden transitions.[82,89,90] $Cs_2InBiCl_6$ and $Cs_2InSbCl_6$ have direct bandgaps and strong optical absorptions, but they tend to decompose spontaneously due to $In^+ \rightarrow In^{3+}$ oxidation.[80,91]

In this review, we summarize our recent computational investigations into the high-throughput screening and materials design of solar-cell materials, and provide comparisons with experimental works.[77,78,92–95] Firstly, chalcogenides and halides with single perovskite structures were systematically screened, which led to the discovery of some novel materials. Secondly, sulfide and halide double perovskites were also comprehensively researched through the cationic chemical mutations of the single perovskite structures. Lastly, spinel and skutterudite compounds that have structures beyond those of perovskites were also examined as solar-cell materials using high-throughput screening methods.

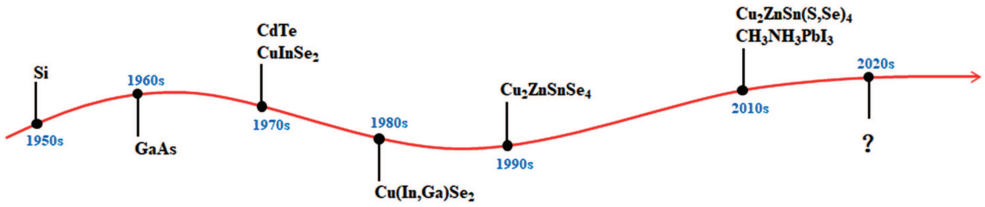


Fig. 1. Diagram showing progress in solar-cell material development.

2. Procedures and criteria for the computational high-throughput screening methodology

The optoelectronic conversion process is shown in Fig. 2. Semiconductors absorb sunlight and generate electrons and holes in the conduction and valence bands, respectively. These electrons and holes undergo complicated processes that include relaxation, recombination, trapping, and transportation. As a result, an optimal solar-cell absorber needs to meet strict requirements, including an appropriate bandgap (1.0–1.6 eV), band alignment, carrier mobility, optical absorption, and high dopability, among others, which are the criteria for the high-throughput screening of solar-cell absorbers. These material properties are associated with various degrees of computational difficulty and cost (as listed in Table 1), and therefore need to be treated in different ways.

A schematic depicting the screening process is shown in Fig. 3, with a chalcogenide single perovskite as the example.

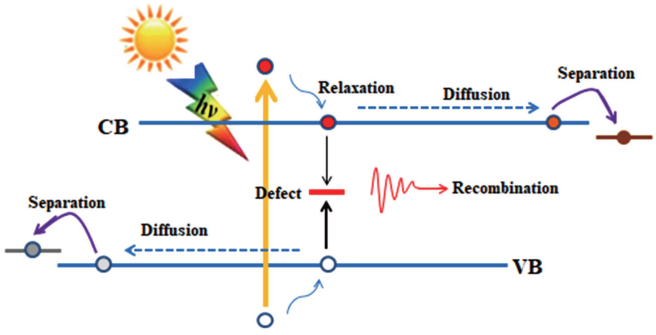


Fig. 2. Schematic diagram of optoelectric conversion process.

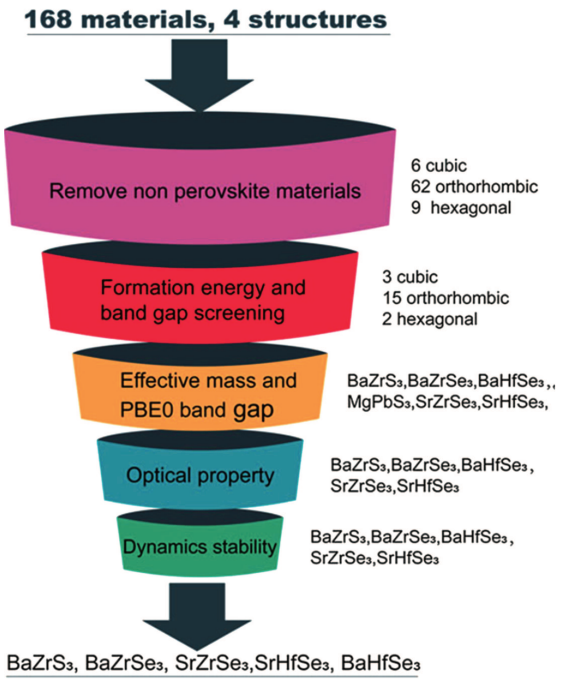


Fig. 3. The screening procedure for novel chalcogenide single perovskites for solar-cell applications. Reprinted with permission.[92]

Table 1. Selected physical quantities for various physical processes, their computational difficulty, cost, and accuracy.

Physical properties			Computational cost	Computational accuracy
Stability	thermodynamic	ΔH_{D}	low	high
	dynamic	phonon spectrum	medium	high
Optical properties	bandgap	PBE	low	low
		HSE	medium	medium
		GW	high	high
	band alignment		high	medium
	optical absorption		low	high
	SLME		low	high
Electronic properties	effective mass		low	high
	carrier mobility		high	low
	diffusion length		high	low
	nonradiative recombination rate		high	low
	defect and doping		medium	medium

2.1. Stability

2.1.1. The stability descriptor

The tolerance factor $t = (R_A + R_x)/\sqrt{2}(R_B + R_x)$[96] and the octahedral factor $\mu = R_B/R_x$ are used to distinguish perovskites, which are formed at $0.8 < t < 1.0$.[97–99] This criterion is insufficiently accurate because t only describes the stability of the structural framework. Recently, we introduced $\mu + t = C$ and $(\mu + t)^{\eta}$ as stability descriptors, where C is a constant and η is the atomic packing fraction. In particular, the $(\mu + t)^{\eta}$ descriptor was shown to be 90% accurate.[77,100,101] These straightforward descriptors can be used to qualitatively screen and select stable perovskites, however, quantitative results are usually obtained by first-principles calculations.

2.1.2. Thermodynamic stability

The development of first-principles computational methods has set the decomposition energy as a quantitative criterion to describe the thermodynamic stability of a material. The decomposition energy is defined as

$$\Delta H_{\mathrm{D}}(\mathrm{material}) = \sum E_{\mathrm{product}} - E_{\mathrm{material}}, \tag{1}$$

where E_{material} is the total energy of the material, E_{product} is the energy of the decomposed products, ΔH_{D} is the energy difference between the material and the corresponding decomposed product. The positive/negative value of ΔH_{D} indicates that the compound is stable/unstable.

2.1.3. Dynamic stability

Dynamic stability can be evaluated from the phonon spectrum.[99,102–104] High-throughput phonon spectra are difficult to calculate because the calculations involved are relatively computationally intensive. Therefore, dynamic stabilities are usually examined in the final round of the screening process.

2.2. Bandgap

The bandgap is a key factor that determines the properties of a material, and about 1.0–1.6 eV is the optimal range for solar absorbers according to the Shockley–Queisser limit.[105] Hybrid functional calculations are computationally demanding, hence the Perdew–Burke–Ernzerhof (PBE) functional is often initially used.[106] Because the PBE functional underestimates the bandgaps, a PBE-calculated 0–1.1 eV bandgap is used as the preliminary screening criterion,[107] with hybrid functional calculations considered for further screening. Apart from the hybrid functional approach, GW[108,109] calculations provide data that agree well with experiment results, but at a higher computational cost.

2.3. Effective mass

Carrier mobility, which is linked to the carrier effective mass and average scattering time, is directly related to photogenerated carrier separation and transportation. Since average scattering time is difficult to calculate, the effective mass is often used as a descriptor for carrier mobility. The effective mass of an electron (hole) is approximately calculated by

$$m^* = \hbar^2 \left[\frac{\partial^2 \varepsilon(k)}{\partial^2 k} \right]^{-1}, \tag{2}$$

where $\varepsilon(k)$ is the energy-dispersion function at the band edges.[92]

2.4. Optical absorption

The absorption coefficient as a function of photon energy is calculated using the expression

$$a(E) = \frac{4\pi e}{hc} \left\{ \frac{\left[\varepsilon_1^2 + \varepsilon_2^2\right]^{1/2} - \varepsilon_1}{2} \right\}, \tag{3}$$

where $\varepsilon(\omega)$ is the frequency-dependent dielectric function

$$\varepsilon(\omega) = \varepsilon_1(\omega) + \mathrm{i}\varepsilon_2(\omega). \tag{4}$$

Due to the high computational cost, the optical absorption spectra are usually calculated using the PBE functional, the calculated spectrum is then shifted to reproduce the bandgap based on the hybrid functional or GW approach. The maximum PCE of a material is determined using the spectroscopic

limited maximum efficiency (SLME) approach.[110,111] Notably, we did not consider exciton binding energy which usually reduces the band gap.[59]

3. Single perovskites

3.1. Chalcogenide perovskites

The high-throughput first-principles calculational method has been used to comprehensively study 168 chalcogenide single perovskites (ABX_3, A = Mg, Ca, Sr, Ba, Zn, Cd, Sn, Pb, B = Ti, Zr, Hf, Si, Ge, Sn, Pb, X = O, S, Se).[92] There are a total of 672 systems for four possible crystal symmetries, namely, $Pm\bar{3}m$, $Pnma$, $P63/mmc$, and $Pnma$ (needle-like). Rough screening with the PBE functional was used to calculate the formation energies and bandgaps, which led to the selection of only a dozen or so materials, as shown in Fig. 4, most of these materials exhibit direct bandgaps, which are favorable for absorbers. Seven materials were retained on the basis of their effective electron (hole) masses, and their bandgaps were calculated using the PBE0 functional, as shown in Fig. 4(b). Finally, $BaZrS_3$, $BaHfSe_3$, $SrZrSe_3$, $SrHfSe_3$, and $BaZrSe_3$ were selected for potential solar-cell applications based on their optical absorption and phonon spectra. The optical absorptions of these materials are comparable to that of $CH_3NH_3PbI_3$, since their band-edge optical absorptions result from the p–d transitions, which have even higher joint densities of states compared to the sp–p transitions observed in $CH_3NH_3PbI_3$.

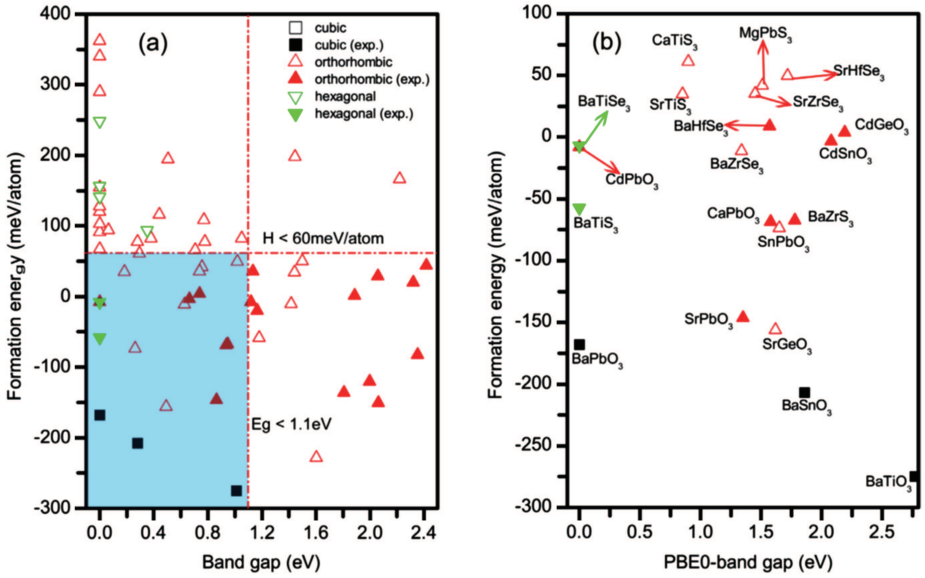


Fig. 4. (a) Formation energies and PBE-calculated bandgaps. (b) Formation energies and PBE0-calculated bandgaps of 20 perovskites. Solid symbols indicate compounds that have been synthesized experimentally. Reprinted with permission.[92]

3.2. Halide single perovskites

Halide single perovskites (ABX_3, A = NH_4, MA (CH_3NH_3), FA ($CH(NH)_2)_2$), Na, K, Rb, Cs, B = Sn, Ge, X = Cl, Br, I) have been extensively researched.[78,112–114] Through the use of high-throughput DFT calculations, we expanded this perovskite family to include another 30 ABX_3 halides (A = Cs, B = Mg, Ca, Sr, Ba, Zn, Cd, Hg, Ge, Sn, Pb, X = Cl, Br, I) with three crystal phases (α, β, and γ). Figure 5 shows the process used to screen the decomposition energy and PBE-calculated bandgap, more details will be published elsewhere. Based on the stability, bandgap, carrier effective mass, and optical absorption, $CsCdBr_3$ shows potential as a solar-cell absorber to replace $CsPbI_3$, despite that $CsCdBr_3$ is also potentially toxic.

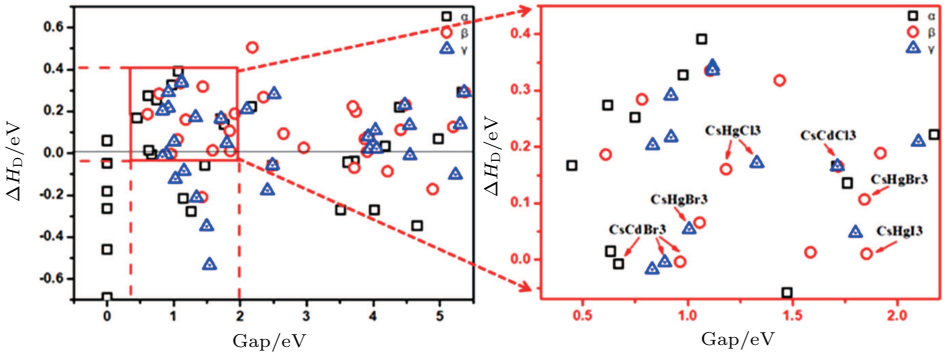


Fig. 5. Decomposition energies and PBE-calculated bandgaps.

4. Double perovskites

4.1. Halide double perovskites

Halide double perovskites $A_2B'B''X_6$ can be considered to have the ABX_3 formula in which the B-cation is split into B' and B''. The compositional flexibility of B' and B'' leads to a very large number of possible candidates. A total of 9520 possible combinations were obtained based on a $7\times8\times34\times5$ system, as shown in Fig. 6.[79] After applying the t and μ rules, this large number was reduced to about 600.[78] We next considered the other screening criteria and found that the remaining candidate materials were mainly grouped into two categories: $Cs_2M(IB)M(III)X_6$ ($M(IB)$ = Cu, Ag, $M(III)$ = Sb, Bi, X = Cl, Br, I), and $Cs_2M(IB)M(III)X_6$ ($M(IB)$ = Cu, Ag, $M(III)$ = Ga, In, X = Cl, Br, I).[78]

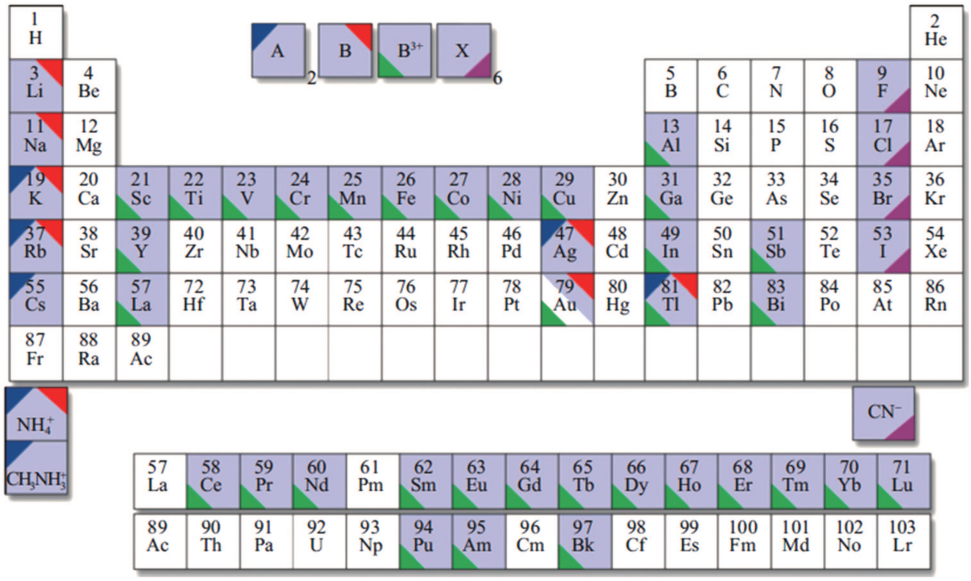


Fig. 6. Elements that from double halide perovskites with the $A_2B^{1+}B^{3+}X_6$ composition. Light blue element indicates that at least one compound with a double halide perovskites structure containing that element has been synthesized. The triangular color tag indicates the site occupied by that element, according to the legend at the top. Au is half-colored because it exists only in $A_2Au_2X_6$ with A = Rb, Cs and X = Cl, Br, I. Reprinted with permission.[79]

$Cs_2AgBiBr_6$ is a representative halide double perovskite from the first category and has been synthesized by McClure and Slavney.[83–85] Some of its superior electronic properties are due to the lone-pair s electrons of Bi, which are similar to the lone-pair s electrons of Pb in $MAPbI_3$. However, $Cs_2AgBiBr_6$ exhibits indirect bandgaps (1.8–2.2 eV) due to the chemical mismatch between Ag and Bi. Meanwhile, its indirect bandgap is favorable for ensuring a long carrier recombination lifetime. $Cs_2AgBiBr_6$ has lower electron ($0.37m_e$) and hole ($0.14m_e$) effective masses than its Pb analog. Meanwhile, $Cs_2AgBiBr_6$ exhibits benign defect properties, and the Ag vacancies are shallow acceptors with low formation energies, which leads to unintended self-doping p-type conductivity. Another representative of this category is $Cs_2AgInCl_6$,[82,89,90] which was first synthesized by Volonakis in 2017. This compound has no lone-pair s electrons, and exhibits direct bandgaps (2.0 eV), however, its optical bandgap is 3.3 eV owing to a parity-forbidden transition between the band edges, which hinders its application to solar cells.

4.2. Chalcogenide double perovskites

Chalcogenides are more stable than halides because Coulombic interactions in chalcogenides are larger than those in ionic halides.[93,100,115] $A_2M(III)M(V)X_6$ chalcogenide double perovskites based on $BaZrS_3$ were generated by the $Zr^{2+}\rightarrow M(III)+M(V)$ chemical mutation. Considering that the lone-pair s electrons play crucial roles in the superior performance of $MAPbI_3$ ($M(III)=Sb^{3+}$, Bi^{3+} and $M(V)=V^{5+}$, Nb^{5+}, Ta^{5+}), lone-pair s electrons can be introduced, as shown in Fig. 7(g), where A = Ca, Sr, Ba and X = S, Se, which leads to 36 chalcogenides with different space groups, as shown in Fig. 7. These compounds were comprehensively investigated using various screening criteria by high-throughput DFT calculations. Among them, nine compounds were selected as candidates for solar-cell applications. Figure 8 shows the decomposition energies of the 9 selected double perovskites through 11 representative pathways. They exhibit quasi-direct bandgaps (indirect bandgap is less than direct bandgap, but the difference between them is very small, $\Delta E_g = E_g^{dir} - E_g^{indir}$), $\Delta E_g < 0.2$ eV, that facilitate electron–hole separation and avoid fast recombination. The conduction band minimum (CBM) is derived from $M(III)$ np–anionic X 3p/4p and $M(V)$ md–X 3p/4p mixing, and the valence band maximum (VBM) is derived from the antibonding state between the $M(III)$ ns and anionic X 3p/4p states, which leads to balanced electron and hole effective masses. The strong antibonding character at both the VBM and CBM leads to strong absorption strengths in the visible-light region, much stronger than that of GaAs, and even stronger than that of $MAPbI_3$.

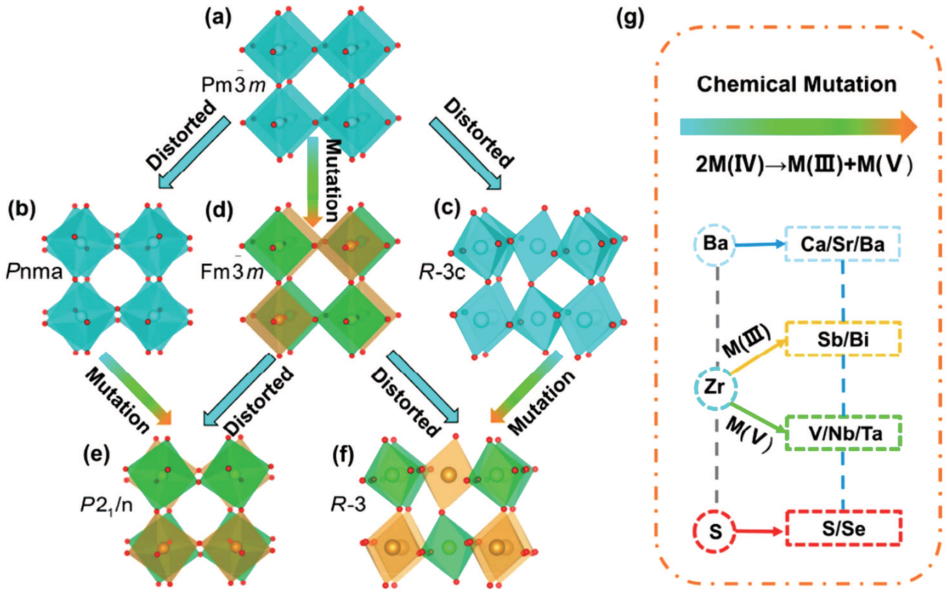


Fig. 7. Schematic crystal structures of (a) $Pm\bar{3}m$ symmetry, (b) *Pnma* symmetry, (c) $R\bar{3}c$ symmetry, (d) $Fm\bar{3}m$ symmetry, (e) $P2_1/n$ symmetry, and (f) $R\bar{3}$ symmetry. Panel (g) shows the chemical mutation of 36 chalcogenide double perovskites from $BaZrS_3$. Reprinted with permission.[93]

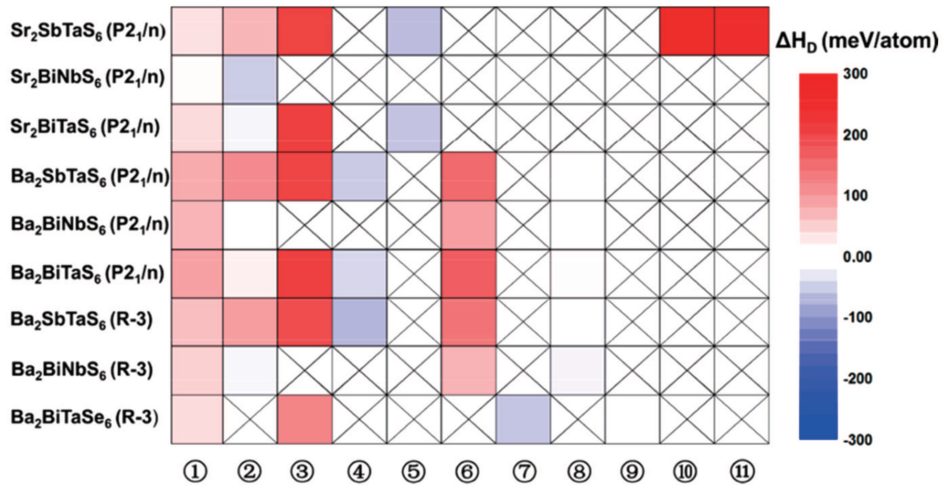


Fig. 8. Heat map of decomposition energies (ΔH_D) for 9 compounds along 11 decomposition pathways. The pathways were determined by searching all related secondary phases in the Inorganic Crystal Structure Database (ICSD). Crosses indicate that the particular pathway does not apply due to the absence of the corresponding secondary phase in the ICSD. Reprinted with permission.[93]

5. Beyond perovskites

5.1. AB_2X_4 spinel compounds

Considering that tetrahedral coordination structures (TCS, e.g., Si, GaAs, and CdTe) and octahedral coordination structures (OCS, e.g., perovskites) exhibit complementary properties in terms of stability, optical properties, and defect tolerance, spinel structures (AB_2X_4), which combine TCS and OCS into single crystal structures, were investigated for solar-cell applications, as shown in Fig. 9. High-throughput DFT calculations were used to systematically investigate 105 spinel AB_2X_4 compounds (A = Mg, Ca, Sr, Ba, Zn, Cd, Hg, B = Sc, Y, Al, Ga, In, X = O, S, Se)[94] in three space groups. Figure 9(d) shows the thermodynamic-screening results and compares them with compounds synthesized experimentally. Furthermore, through bandgap, effective-mass, optical-absorption, and dynamic-stability screening, five spinel compounds, namely, $HgAl_2Se_4$, $HgIn_2S_4$, $CdIn_2Se_4$, $HgScS_4$, and HgY_2S_4 were determined to be promising solar-cell absorbers. Among them, $HgAl_2Se_4$ exhibited the most outstanding properties, it has a suitable quasi-direct bandgap (1.36 eV), with $\Delta E_g = 24$ meV. It also has appropriate carrier electron ($0.08m_e$) and hole ($0.69m_e$) effective masses. Moreover, these compounds have strong absorption strengths because their VBMs mainly involve Se/S 9 components, while their CBMs contain Se/S s components.

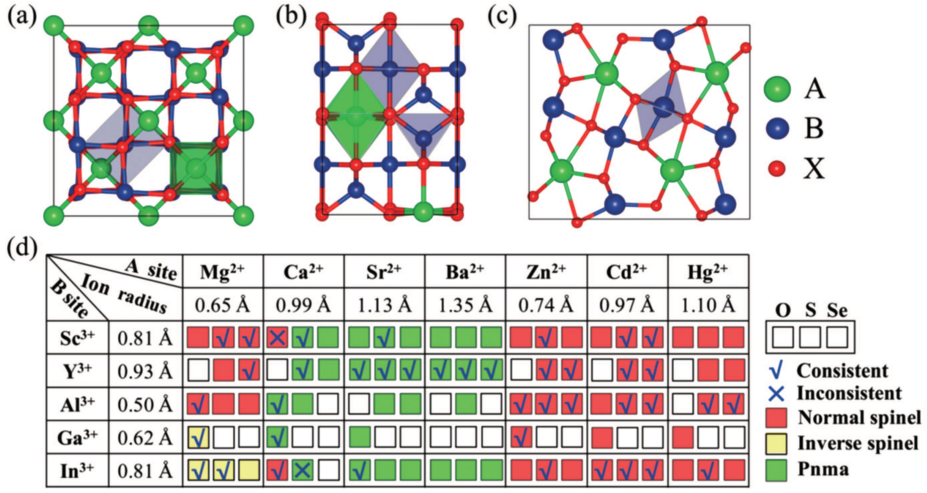


Fig. 9. Crystal structures of (a) spinel, (b) inverse spinel, and (c) distorted *Pnma* phases. The *A* and *B* polyhedra are shown in green and blue, respectively. (d) DFT-calculated and experimental phase stabilities of 105 AB_2X_4 compounds. Red, yellow, and green squares indicate that spinel, inverse spinel, and *Pnma* phases are calculated to be stable structures, respectively. Ticks (crosses) indicate that the theoretical predictions are consistent (inconsistent) with existing experimental ICSD data. Reprinted with permission.[94]

5.2. Skutterudite compounds

The materials in the preceding sections were selected on the basis of their structural characteristics or electronic properties for conventional solar-cell absorber applications. However, the $IrSb_3$ skutterudite, which lies out of the scope of ns^2-containing compounds,[55] has also been proposed to be a promising solar-cell material.[95] The structure and electronic structure of $IrSb_3$ are shown in Fig. 10, along with that of perovskite. $IrSb_3$ has an appropriate direct bandgap ($\sim$ 1.3 eV), and small carrier electron ($0.11m_e$) and hole ($0.07m_e$) effective masses. Its high absorption strength is comparable to that of $MAPbI_3$. Moreover, it presents shallow dominating defects. These superior qualities are mainly derived from the strong antibonding character at the VBM, however, lone-pair s electrons make no contribution to the VBM. Furthermore, $IrSb_3$ is highly stable due to its covalent nature.

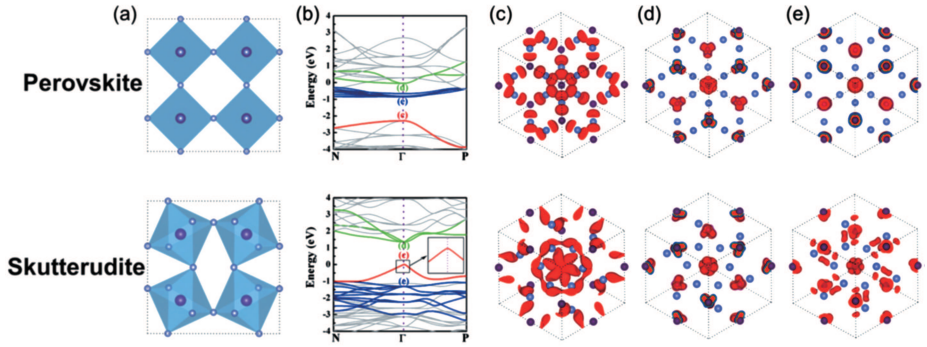


Fig. 10. (a) Crystal structures, (b) band structures, and their respective partial charge densities: (c) VBM, (d) CBM, and (e) the blue bands indicated in the band structures in panel (b). The almost linear band structure around the VBM (5% length along Γ–N and Γ–P) of skutterudite is shown in the inset of panel (b). Reprinted with permission.[95]

6. Conclusions and perspectives

The design of new materials is mainly driven by structural and functional-property requirements. By considering structural diversity and compositional flexibility, there appears to be tens of millions of possible new materials. In this paper, we reviewed progress toward the discovery of new solar-cell materials using high-throughput calculations, which have proven to be powerful methods for the screening and design of solar-cell materials. The materials examined were mainly divided into three categories: single perovskites, double perovskites, and beyond perovskites. Some promising candidates for solar-cell materials were discovered, such as single perovskites $BaZrS_3$, $CsPbI_3$, double perovskite Ba_2BiNbS_6, spinel $HgAl_2Se_4$, and skutterudite $IrSb_3$, among others, these compounds exhibit superior properties for solar-cell applications, including high stabilities, appropriate bandgaps, small carrier effective masses, extremely high optical absorptions, and benign defect properties. It is worth noting that $CsPbI_3$ and $HgAl_2Se_4$ are still potentially toxic, they involve the toxic elements Pb and Hg. These results provide strong guidelines for the experimental synthesis of new materials. However, as mentioned above, a vast domain of materials exist that await discovery. The search for stable, non-toxic, inexpensive, and highly efficient solar-cell materials remains a hot

topic. Recently, machine learning based on the data from high-throughput calculations has opened up a new approach to the efficient screening and design of solar-cell materials.

Acknowledgments

The work was carried out at the National Supercomputer Center in Tianjin, and the calculations were performed on TinaH-1(A).

References

[1] Armand M and Tarascon J M 2008 *Nature* **451** 652
[2] Gasteiger H A and Marković N M 2009 *Science* **324** 48
[3] Cook T R, Dogutan D K, Reece S Y, Surendranath Y, Teets T S and Nocera D G 2010 *Chem. Rev.* **110** 6474
[4] Green M A and Bremner S P 2017 *Nat. Materials* **16** 23
[5] Yin W J, Weng B, Ge J, Sun Q, Li Z and Yan Y 2019 *Energy & Environ. Sci.* **12** 442
[6] Repins I, Contreras M, Romero M, Yan Y, Metzger W, Li J, Johnston S, Egaas B, DeHart C and Scharf J *2008 33rd IEEE Photovoltaic Specialists Conference* p. 1
[7] Palik E D 1998 *Handbook Optical Constants Solids* Vol. 3 (New York: Academic Press)
[8] De Wolf S, Holovsky J, Moon S J, Löper P, Niesen B, Ledinsky M, Haug F J, Yum J H and Ballif C 2014 *J. Phys. Chem. Lett.* **5** 1035
[9] Deng H X, Luo J W and Wei S H 2018 *Chin. Phys. B* **27** 117104
[10] Deng H X, Wei S H, Li S S, Li J and Walsh A 2013 *Phys. Rev. B* **87** 125203
[11] Cahen D and Noufi R 1989 *Appl. Phys. Lett.* **54** 558
[12] Zhang L, Da Silva J L, Li J, Yan Y, Gessert T and Wei S H 2008 *Phys. Rev. Lett.* **101** 155501
[13] Jha A R 2009 *Solar cell technology and applications* (New York: Auerbach Publications)
[14] Rau U, Taretto K and Siebentritt S 2009 *Appl. Phys. A* **96** 221
[15] Zhang S, Wei S H, Zunger A and Katayama-Yoshida H 1998 *Phys. Rev. B* **57** 9642
[16] Chen S, Walsh A, Gong X G and Wei S H 2013 *Adv. Mater.* **25** 1522
[17] Chen S, Gong X, Walsh A and Wei S H 2010 *Appl. Phys. Lett.* **96** 021902
[18] Körbel S, Kammerlander D, Sarmiento-Pérez R, Attaccalite C, Marques M A and Botti S 2015 *Phys. Rev. B* **91** 075134
[19] Park J S, Kim S, Xie Z and Walsh A 2018 *Nat. Rev. Mater.* **3** 194
[20] Yin W J, Wu Y, Wei S H, Noufi R, Al-Jassim M M and Yan Y 2014 *Adv. Energy Mater.* **4** 1300712
[21] Green M A, Emery K, Hishikawa Y, Warta W and Dunlop E D 2015 *Prog. Photovoltaics: Research Applications* **23** 1
[22] Walsh A, Payne D J, Egdell R G and Watson G W 2011 *Chem. Soc. Rev.* **40** 4455
[23] Shah A, Torres P, Tscharner R, Wyrsch N and Keppner H 1999 *Science* **285** 692
[24] Kojima A, Teshima K, Shirai Y and Miyasaka T 2009 *J. Am. Chem. Soc.* **131** 6050
[25] Lee B, He J, Chang R P and Kanatzidis M G 2012 *Nature* **485** 486
[26] Lee M M, Teuscher J, Miyasaka T, Murakami T N and Snaith H J 2012 *Science* **338** 643
[27] Kim H S, Lee C R, Im J H, Lee K B, Moehl T, Marchioro A, Moon S J, Humphry-Baker R, Yum J H and Moser J E 2012 *Sci. Rep.* **2** 591
[28] Etgar L, Gao P, Xue Z, Peng Q, Chandiran A K, Liu B, Nazeeruddin M K and Grätzel M 2012 *J. Am. Chem. Soc.* **134** 17396
[29] Kim H S, Lee J W, Yantara N, Boix P P, Kulkarni S A, Mhaisalkar S, Grätzel M and Park N G 2013 *Nano Lett.* **13** 2412
[30] Edri E, Kirmayer S, Cahen D and Hodes G 2013 *J. Phys. Chem. Lett.* **4** 897
[31] Cai B, Xing Y, Yang Z, Zhang W H and Qiu J 2013 *Energy & Environ. Sci.* **6** 1480
[32] Burschka J, Pellet N, Moon S J, Humphry-Baker R, Gao P, Nazeeruddin M K and Grätzel M 2013 *Nature* **499** 316
[33] Bisquert J 2013 *The swift surge of perovskite photovoltaics* (New York: ACS Publications)
[34] Liu M, Johnston M B and Snaith H J 2013 *Nature* **501** 395
[35] Noh J H, Im S H, Heo J H, Mandal T N and Seok S I 2013 *Nano Lett.* **13** 1764
[36] Gao P, Grätzel M and Nazeeruddin M K 2014 *Energy & Environ. Sci.* **7** 2448
[37] Green M A, Ho-Baillie A and Snaith H J 2014 *Nat. Photon.* **8** 506
[38] Bretschneider S A, Weickert J, Dorman J A and Schmidt-Mende L 2014 *APL Mater.* **2** 040701
[39] Snaith H J 2013 *J. Phys. Chem. Lett.* **4** 3623
[40] Park N G 2013 *J. Phys. Chem. Lett.* **4** 2423
[41] Stranks S D, Eperon G E, Grancini G, Menelaou C, Alcocer M J, Leijtens T, Herz L M, Petrozza A and Snaith H J 2013 *Science* **342** 341
[42] Xing G, Mathews N, Sun S, Lim S S, Lam Y M, Grätzel M, Mhaisalkar S and Sum T C 2013 *Science* **342** 344
[43] McGehee M D 2013 *Nature* **501** 323
[44] McGehee M D 2014 *Nat. Mater.* **13** 845
[45] Nie W, Tsai H, Asadpour R, Blancon J C, Neukirch A J, Gupta G, Crochet J J, Chhowalla M, Tretiak S and Alam M A 2015 *Science* **347** 522
[46] Li X, Bi D, Yi C, Décoppet J D, Luo J, Zakeeruddin S M, Hagfeldt A and Grätzel M 2016 *Science* **353** 58
[47] Grancini G, D'Innocenzo V, Dohner E R, Martino N, Kandada A S, Mosconi E, De Angelis F, Karunadasa H, Hoke E and Petrozza A 2015 *Chem. Sci.* **6** 7305
[48] Senthilarasu S, Fernández E F, Almonacid F and Mallick T K 2015 *Sol. Energy Mater. Sol. Cells* **133** 92
[49] Stranks S D, Nayak P K, Zhang W, Stergiopoulos T and Snaith H J 2015 *Angew. Chem. Int. Ed.* **54** 3240
[50] Green M A and Bein T 2015 *Nat. Mater.* **14** 559
[51] Stranks S D and Snaith H J 2015 *Nat. Nanotech.* **10** 391
[52] Grätzel M 2014 *Nat. Mater.* **13** 838
[53] Zhou H, Chen Q, Li G, Luo S, Song T B, Duan H S, Hong Z, You J, Liu Y and Yang Y 2014 *Science* **345** 542
[54] Saliba M, Matsui T, Domanski K, Seo J Y, Ummadisingu A, Zakeeruddin S M, Correa-Baena J P, Tress W R, Abate A and Hagfeldt A 2016 *Science* **354** 206
[55] Yin W J, Shi T and Yan Y 2014 *Appl. Phys. Lett.* **104** 063903
[56] Buin A, Pietsch P, Xu J, Voznyy O, Ip A H, Comin R and Sargent E H 2014 *Nano Lett.* **14** 6281
[57] Ganose A M, Savory C N and Scanlon D O 2017 *Chem. Commun.* **53** 20
[58] Stoumpos C C, Malliakas C D and Kanatzidis M G 2013 *Inorg. Chemistry* **52** 9019
[59] Zhang F, Castaneda J F, Chen S, Wu W, DiNezza M J, Lassise M, Nie W, Mohite A, Liu Y and Liu S 2019 arXiv:1907.03434 [physics.app-ph]
[60] Yin W J, Shi T and Yan Y 2014 *Adv. Mater.* **26** 4653
[61] Yin W J, Yang J H, Kang J, Yan Y and Wei S H 2015 *J. Mater. Chem. A* **3** 8926
[62] Babayigit A, Ethirajan A, Muller M and Conings B 2016 *Nat. Mater.* **15** 247
[63] Hailegnaw B, Kirmayer S, Edri E, Hodes G and Cahen D 2015 *J. Phys. Chem. Lett.* **6** 1543
[64] Babayigit A, Thanh D D, Ethirajan A, Manca J, Muller M, Boyen H G and Conings B 2016 *Sci. Rep.* **6** 18721
[65] Wang P, Zhang X, Zhou Y, Jiang Q, Ye Q, Chu Z, Li X, Yang X, Yin Z and You J 2018 *Nat. Commun.* **9** 2225
[66] Swarnkar A, Marshall A R, Sanehira E M, Chernomordik B D, Moore D T, Christians J A, Chakrabarti T and Luther J M 2016 *Science* **354** 92
[67] Eperon G E, Paterno G M, Sutton R J, Zampetti A, Haghighirad A A, Cacialli F and Snaith H J 2015 *J. Mater. Chem. A* **3** 19688
[68] Kim Y G, Kim T Y, Oh J H, Choi K S, Kim Y J and Kim S Y 2017 *Phys. Chem. Chem. Phys.* **19** 6257
[69] Frolova L A, Anokhin D V, Piryazev A A, Luchkin S Y, Dremova N N, Stevenson K J and Troshin P A 2016 *J. Phys. Chem. Lett.* **7** 4353
[70] Dastidar S, Hawley C J, Dillon A D, Gutierrez-Perez A D, Spanier J E and Fafarman A T 2017 *J. Phys. Chem. Lett.* **8** 1278
[71] Chen C Y, Lin H Y, Chiang K M, Tsai W L, Huang Y C, Tsao C S and Lin H W 2017 *Adv. Mater.* **29** 1605290
[72] Huang Y, Yin W J and He Y 2018 *J. Phys. Chem. C* **122** 1345
[73] Ye Q, Zhao Y, Mu S, Ma F, Gao F, Chu Z, Yin Z, Gao P, Zhang X and You J 2019 *Adv. Mater.* **31** 1905143

[74] Yue M, Su J, Zhao P, Lin Z, Zhang J, Chang J and Hao Y 2019 *Nano-Micro Lett.* **11** 91
[75] Chen H, Guo A, Gu X and Feng M 2019 *J. Alloys Compd.* **789** 392
[76] Zhang L, Cui W, Zang Z, Tian F, Li X and Qin G 2019 *Sol. Energy* **188** 224
[77] Li Z, Xu Q, Sun Q, Hou Z and Yin W J 2019 *Adv. Funct. Mater.* **29** 1807280
[78] Li Z and Yin W 2018 *J. Semicond.* **39** 071003
[79] Giustino F and Snaith H J 2016 *ACS Energy Lett.* **1** 1233
[80] Xiao Z, Du K Z, Meng W, Wang J, Mitzi D B and Yan Y 2017 *J. Am. Chem. Soc.* **139** 6054
[81] Xiao Z, Du K Z, Meng W, Mitzi D B and Yan Y 2017 *Angew. Chem.* **129** 12275
[82] Meng W, Wang X, Xiao Z, Wang J, Mitzi D B and Yan Y 2017 *J. Phys. Chem. Lett.* **8** 2999
[83] McClure E T, Ball M R, Windl W and Woodward P M 2016 *Chem. Mater.* **28** 1348
[84] Slavney A H, Hu T, Lindenberg A M and Karunadasa H I 2016 *J. Am. Chem. Soc.* **138** 2138
[85] Volonakis G, Filip M R, Haghighirad A A, Sakai N, Wenger B, Snaith H J and Giustino F 2016 *J. Phys. Chem. Lett.* **7** 1254
[86] Filip M R, Hillman S, Haghighirad A A, Snaith H J and Giustino F 2016 *J. Phys. Chem. Lett.* **7** 2579
[87] Savory C N, Walsh A and Scanlon D O 2016 *ACS Energy Lett.* **1** 949
[88] Greul E, Petrus M L, Binek A, Docampo P and Bein T 2017 *J. Mater. Chem. A* **5** 19972
[89] Volonakis G, Haghighirad A A, Milot R L, Sio W H, Filip M R, Wenger B, Johnston M B, Herz L M, Snaith H J and Giustino F 2017 *J. Phys. Chem. Lett.* **8** 772
[90] Tran T T, Panella J R, Chamorro J R, Morey J R and McQueen T M 2017 *Mater. Horizons* **4** 688
[91] Zhao X G, Yang J H, Fu Y, Yang D, Xu Q, Yu L, Wei S H and Zhang L 2017 *J. Am. Chem. Soc.* **139** 2630
[92] Huo Z, Wei S H and Yin W J 2018 *J. Phys. D: Appl. Phys.* **51** 474003
[93] Sun Q, Chen H and Yin W J 2018 *Chem. Mater.* **31** 244
[94] Wang J, Chen H, Wei S H and Yin W J 2019 *Adv. Mater.* **31** 1806593
[95] Yin Y, Huang Y, Wu Y, Chen G, Yin W J, Wei S H and Gong X 2017 *Chem. Mater.* **29** 9429
[96] Goldschmidt V 1926 *Naturwissenschaften* **14** 477
[97] Li C, Soh K C K and Wu P 2004 *J. Alloys Compd.* **372** 40
[98] Li C, Lu X, Ding W, Feng L, Gao Y and Guo Z 2008 *Acta Crystallogr. Sect. B: Struct. Sci.* **64** 702
[99] Baroni S, De Gironcoli S, Dal Corso A and Giannozzi P 2001 *Rev. Mod. Phys.* **73** 515
[100] Sun Q and Yin W J 2017 *J. Am. Chem. Soc.* **139** 14905
[101] Xu Q, Li Z, Liu M and Yin W J 2018 *J. Phys. Chem. Lett.* **9** 6948
[102] Giannozzi P, De Gironcoli S, Pavone P and Baroni S 1991 *Phys. Rev. B* **43** 7231
[103] Gonze X and Lee C 1997 *Phys. Rev. B* **55** 10355
[104] Togo A and Tanaka I 2015 *Scr. Mater.* **108** 1
[105] Shockley W and Queisser H J 1961 *J. Appl. Phys.* **32** 510
[106] Heyd J, Scuseria G E and Ernzerhof M 2003 *J. Chem. Phys.* **118** 8207
[107] Perdew J P, Burke K and Ernzerhof M 1996 *Phys. Rev. Lett.* **77** 3865
[108] Shishkin M and Kresse G 2007 *Phys. Rev. B* **75** 235102
[109] Klimeš J, Kaltak M and Kresse G 2014 *Phys. Rev. B* **90** 075125
[110] Yu L and Zunger A 2012 *Phys. Rev. Lett.* **108** 068701
[111] Yu L, Kokenyesi R S, Keszler D A and Zunger A 2013 *Adv. Energy Mater.* **3** 43
[112] Noel N K, Stranks S D, Abate A, Wehrenfennig C, Guarnera S, Haghighirad A A, Sadhanala A, Eperon G E, Pathak S K and Johnston M B 2014 *Energy & Environ. Sci.* **7** 3061
[113] Hao F, Stoumpos C C, Cao D H, Chang R P and Kanatzidis M G 2014 *Nat. Photon.* **8** 489
[114] Hanusch F C, Wiesenmayer E, Mankel E, Binek A, Angloher P, Fraunhofer C, Giesbrecht N, Feckl J M, Jaegermann W and Johrendt D 2014 *J. Phys. Chem. Lett.* **5** 2791
[115] Sun Q, Wang J, Yin W J and Yan Y 2018 *Adv. Mater.* **30** 1705901